

Quantification of fluoroquinolone uptake through the outer membrane channel OmpF of *Escherichia coli*

Jehangir Cama^a, Harsha Bajaj^b, Stefano Pagliara^{a,c}, Theresa Maier^a, Yvonne Braun^b, Mathias Winterhalter^b and Ulrich F. Keyser^{a,*}

Affiliations: a. Biological and Soft Systems, Cavendish Laboratory, Department of Physics, University of Cambridge, JJ Thomson Avenue, Cambridge CB3 0HE, United Kingdom.

b. Jacobs University Bremen, Campus Ring 1, D-28759, Bremen, Germany.

c. Department of Biosciences, College of Life and Environmental Sciences, University of Exeter, Exeter, United Kingdom.

Correspondence: Ulrich F. Keyser, ufk20@cam.ac.uk, +44 (0) 1223 337007.

Decreased drug accumulation is a common cause of antibiotic resistance in microorganisms. However, there are few reliable general techniques capable of quantifying drug uptake through bacterial membranes. We present a semi-quantitative optofluidic assay for studying the uptake of autofluorescent drug molecules in single liposomes. We studied the effect of the *Escherichia coli* outer membrane channel OmpF on the accumulation of the fluoroquinolone antibiotic, norfloxacin, in proteoliposomes. Measurements were performed at pH 5 and pH 7, corresponding to two different charge states of norfloxacin that bacteria are likely to encounter in the human gastrointestinal tract. The optofluidic assay estimates a flux of about 10 norfloxacin molecules per second per OmpF trimer in the presence of a 1 mM concentration gradient of norfloxacin. We also performed single channel electrophysiology measurements and found that the application of transmembrane voltages causes an electric field driven uptake in addition to concentration driven diffusion. We use our results to propose a physical mechanism for the pH mediated change in bacterial susceptibility to fluoroquinolone antibiotics.

Introduction

Antimicrobial resistance is a daunting challenge, threatening to undermine the very fabric of modern medicine today¹⁻⁴. The inexorable emergence of resistant organisms, coupled with a decline in the discovery of new antimicrobials, has led to a global public health crisis. The recent breakthrough discovery of a new antibiotic, teixobactin⁵, is extremely good news. However, its relative inactivity against Gram-negative pathogens shows that the battle against antimicrobial resistance will be extremely challenging.

Gram-negative bacteria have a hydrophobic double-membrane cell wall that presents a barrier for hydrophilic molecules trying to enter the cell. The outer membrane (OM) is even more hydrophobic than a typical phospholipid membrane due to the presence of lipopolysaccharides (LPS), whose strong lateral interactions inhibit the passage of a variety of compounds through the OM⁶. Translocation across the OM is thus mainly governed by the presence of outer membrane protein “porins” that form water-filled channels allowing the diffusion of compounds through the OM.

Consequently, the down-regulation of these porins enables bacteria to escape the deleterious effects of antibiotics⁶⁻⁹. For example, a reduction in the expression of Outer membrane protein F (OmpF), a major porin found in *Escherichia coli*, has been associated with a decrease in the accumulation of fluoroquinolone antibiotics; this eventually gives rise to drug resistance^{7,10-12}. Furthermore, antibiotic therapy results in a switch in porin expression from OmpF to the narrower OmpC; this is thought to be due to the high osmolarity conditions existing in patients under drug treatment⁷. This leads to a significant decrease in antibiotic accumulation within the cell, and hence a decrease in antibiotic susceptibility⁷. It is thus clear that understanding antibiotic accumulation in cells is crucial, and methods to better quantify antibiotic permeation are urgently required¹³.

Fluoroquinolones are broad-spectrum antibiotics that inhibit bacterial type II topoisomerases. These topoisomerases are essential enzymes, involved in key cellular processes such as DNA replication¹⁴. Since their targets are intracellular, fluoroquinolones must pass through the outer and inner bacterial membrane to be effective¹⁰. The OM thus presents the initial diffusion barrier for drug uptake, and the accumulation of fluoroquinolone molecules in the periplasm ultimately determines their flux into the cytoplasm. Changes in bacterial susceptibility to fluoroquinolones due to changes in pH have been reported previously^{15,16}. An increase in external pH from acidic to basic was shown to correspond to a reduction in the minimum inhibitory concentration (MIC) of norfloxacin¹⁷. Further, it was proposed that this pH mediated change in susceptibility is related to changes in the uptake of fluoroquinolones due to alterations of the electric charge of the antibiotic molecule^{18,19}; norfloxacin, for example, is positively charged at pH 5 and neutral (zwitterionic, but a significant proportion are also uncharged) at pH 7^{18,19}. It thus seems reasonable to assume that the fluoroquinolone susceptibility of bacteria in response to pH changes is a complicated process, which might involve both changes in porin expression²⁰ and changes in drug transport through porins in the OM as well as through the phospholipid inner membrane.

At acidic pH values, fluoroquinolone molecules carry charge¹⁸ and thus transport across the OM should be strongly influenced by even relatively small potentials across the OM. Donnan potentials are known to exist across the OM due to the presence of anchored, anionic membrane-derived oligosaccharides (MDOs) in the *E. coli* periplasm^{21,22}. The magnitude of these potentials depends strongly on the ionic concentration of the surrounding medium. At physiological ion concentrations, the Donnan potential is of the order of 20-30 mV, but variations of 5-100 mV have

been reported by changing external cation concentrations²¹. One would expect such changes to have a significant effect on the transport of charged molecules through OM porins.

For autofluorescent antibiotics like quinolones, the determination of antibiotic uptake via a cell ensemble recording has previously been suggested. However, the technique suffers from difficulties in distinguishing between antibiotic molecules that were accumulated inside versus those bound to the cell membrane²³. More recently, fluorescence based single cell imaging enabled the comparison of fleroxacin uptake in resistant versus susceptible bacteria²⁴. However, barring these few exceptions, a quantitative analysis of fluoroquinolone transport through porins and lipids has proven technologically challenging.

In this study we describe an optofluidic assay that measures the permeability of antibiotics through porins exclusively in a proteoliposome system. OmpF porins are reconstituted into giant unilamellar vesicles and norfloxacin uptake into these proteoliposomes is tracked directly in a label-free manner using the UV autofluorescence of the drug. Patching the proteoliposomes reveals an estimate of the porin density, and combining the two measurements enables the calculation of norfloxacin translocation rates through OmpF channels in the proteoliposomes. Furthermore, proteoliposomes are cell-free systems, and thus active or passive uptake processes can be independently examined in highly controlled environments. We compare our measurements with single channel electrophysiology, and explore the combined effect of pH and transmembrane voltage on norfloxacin transport through OmpF.

Results

Optofluidic Permeability Assay

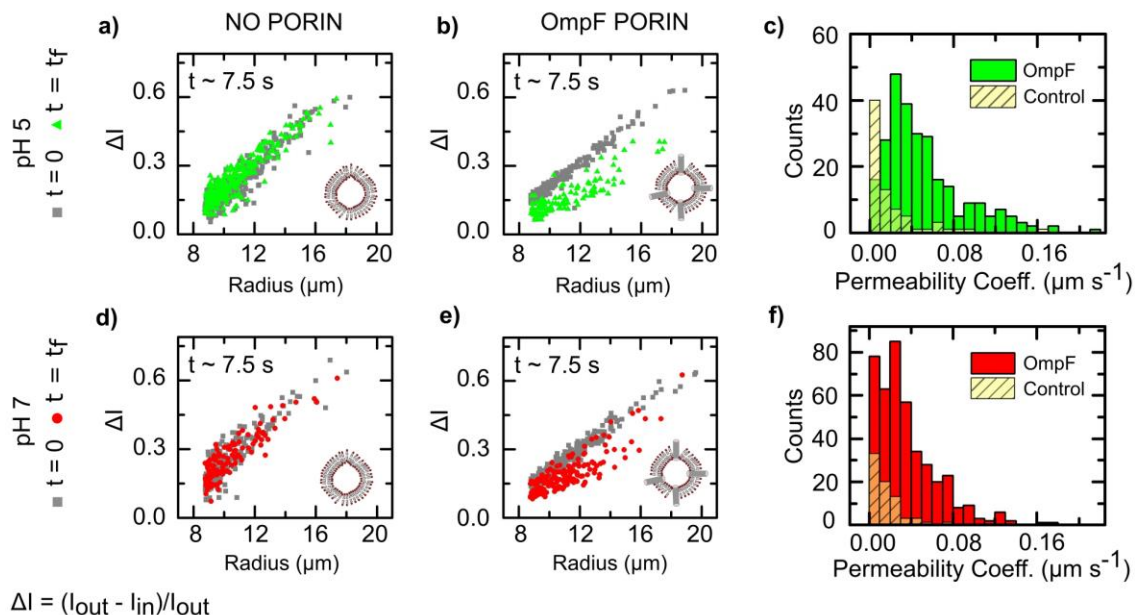


Figure 1. Optofluidic permeability assay shows the rapid uptake of norfloxacin in OmpF embedded proteoliposomes. Comparison of the uptake measurements in liposomes and proteoliposomes at pH 5 (a and b) and pH 7 (d and e). Each point references an uptake measurement at the single vesicle level, the grey points being $t = 0$ and the green (pH 5) and red (pH 7) being the final detection point $t = t_f$. On average it took individual vesicles about 7.5 s to move from the initial to the final detection point. In the

absence of porins (a,d), there is no shift in ΔI values observed at the later time point at either pH. The presence of porins (b,e) leads to a marked downward shift in ΔI for the majority of the proteoliposomes at the later detection point, both at pH 5 and pH 7. The downward shift in ΔI corresponds to an increase in the norfloxacin autofluorescence intensity within the proteoliposome (I_{in}), and is thus a direct measure of norfloxacin uptake. Scatter plots of other porin experiments are presented in the Supplementary Information. The histograms (c,f) are a record of permeability coefficients (P) measured for individual porin-embedded proteoliposomes, and summarise the data from 3 separate experiments at each pH. Histograms from the control measurements with liposomes (no porins) are overlaid to show the shift in P due to the presence of porins in the membrane. Total liposomes/proteoliposomes detected were $N = 268$ (pH 5, with porins), $N = 74$ (pH 5, no porins), $N = 420$ (pH 7, with porins) and $N = 74$ (pH 7, no porins).

In the optofluidic permeability assay, OmpF embedded proteoliposomes (see Methods) are exposed to norfloxacin by controlled mixing in a T junction microfluidic chip. The vesicles (liposomes/proteoliposomes) are imaged under UV irradiation at two points, first immediately post mixing with the drug and then again after time t , a short distance further downstream. A comparison of the drug UV autofluorescence intensities within the vesicles at both points enables the direct visualisation of drug uptake and the calculation of the permeability coefficient (P) and flux (J) of the drug through the vesicle membrane. This assay also allows the comparison of norfloxacin flux values through OmpF at different pH conditions in the absence of an applied transmembrane voltage.

The results of the optofluidic permeability assay are summarised in Figure 1 – more results can be viewed in the Supplementary Information Figure S1. The graphs (Figures 1 a,b,d,e) show a normalised intensity difference ($\Delta I = \{(I_{out} - I_{in})/I_{out}\}$) between the background autofluorescence intensity (I_{out}) and the autofluorescence intensity inside the vesicle (I_{in}), versus vesicle radius (R). Each point represents a single vesicle measurement. The grey squares represent vesicles at the initial viewpoint immediately post mixing with the norfloxacin (which for convenience we set to $t = 0$). The green triangles (pH 5) and red circles (pH 7) represent vesicles once they have travelled along the channel to the next detection position. The Permeability Coefficient (P) is given by²⁵:

$$P = -\left(\frac{R}{3t}\right) \times \ln(\Delta I(t) - \Delta I(0) + 1)$$

where t is the time taken for the vesicle to move from the initial detection point to the final detection point (on average this was about 7.5 s). The norfloxacin concentration present in the channel after mixing is about 1 mM; at $t = 0$, there is no norfloxacin inside the vesicles, whereas outside the vesicles the concentration is 1 mM.

The experiments were performed at pH 5 and pH 7. In both cases the presence of OmpF causes a marked change in ΔI indicating the rapid accumulation of the drug inside the proteoliposomes.

Control measurements in the absence of OmpF revealed a substantially slower uptake, indicating that OmpF porins significantly enhance the permeability of the membranes to norfloxacin. We can calculate the contributions to the flux from the porins and lipids separately; details are given in the Supplementary Information. In contrast to permeation in the absence of OmpF²⁵, the presence of the porins leads to similar permeability coefficients at both pH 5 and pH 7. The relative pH independence suggests that the charge of the molecule does not play a significant role in influencing its transport through the porin in the absence of a transmembrane potential.

The spread in the permeability coefficient histograms (Figure 1 c,f) is caused by the inevitable variability of OmpF insertions into individual vesicles prepared for the optofluidics experiments. This can be seen in the scatter plots as well – it is clear that, at both pH conditions, a handful of

vesicles do not show significant transport. It is known, however, that electroformation produces some multilamellar vesicles²⁶, and in these the porins cannot insert across all membranes; this accounts for the few negative observations.

Norfloxacin Flux Calculation in the Proteoliposomes

To obtain an estimate of the flux per porin from the optofluidics assay, vesicles incubated with OmpF were patched and characterised electrically using a Port-a-Patch system (Nanion Technologies GmbH, Germany) (Supplementary Figure S2). Since the patched area is well-known (patch diameter = 1 μm) and the number of porin insertions counted (using the ionic current characteristics, details in Methods), this calibration measurement established a [porin]:[lipid surface area] ratio for the vesicles. Our results yield an estimate of ~ 2000 porins per μm^2 for the proteoliposomes used in the optofluidics assay. It is interesting to compare this result to the estimated number of general diffusion porins found in a typical bacterial cell; these porins are found in excess of 10^5 copies per cell⁶. This translates into an approximately 6 \times higher [porin]:[lipid surface area] ratio than for our experiments.

The flux of norfloxacin through the vesicle membrane is given by $J = P \times 4\pi R^2 \times \Delta c$. Combining this with the Port-a-Patch measurements, we can calculate the flux per porin on a single proteoliposome basis (full details of the calculation are provided in the Supplementary Information). An average over all the proteoliposomes detected gives a norfloxacin flux value per porin of 10 ± 7 molecules/s (N=420) at pH 7 and 14 ± 9 molecules/s (N=268) at pH 5 (errors are Standard Deviations). The errors are a direct consequence of the variability in OmpF insertion, as seen in the Supplementary Information Figure S2. If we include a correction (details in Supplementary Information) to account for the contribution of flux across the pure lipids²⁵, the change in the final result is negligible - at pH 7 the flux per porin is marginally reduced to 9 ± 7 molecules/s; at pH 5 there is no change.

Antibiotic interaction with OmpF using Single channel electrophysiology

In this assay, electrophysiology was used to study the interaction of norfloxacin with OmpF channels reconstituted in planar lipid bilayers. Traditionally, a lipid bilayer is formed across an aperture in a Teflon film that separates two reservoirs in a cuvette. The reservoirs are filled with an electrolyte solution and a potential difference is applied across the lipid membrane via electrodes in the reservoirs. Porins are reconstituted in the lipid bilayer and their conductance properties studied by measuring the ionic current flowing through the membrane. The addition of antibiotics leads to blockages in the ionic current, since the antibiotic molecules displace ions flowing through the porin. A detailed description of the technique is provided in the Methods section.

We varied the transmembrane voltages (25 mV and 50 mV) to determine whether the charge on the norfloxacin molecule at pH 5 influenced its transport through the channel under an applied electric field comparable to the OM potentials in natural systems. In the absence of antibiotics, fluctuations in the ionic current through a single OmpF channel were negligible, both at pH 7 and pH 5 (Figures 2a and 2c). The addition of 250 μM norfloxacin to the extracellular (*cis*) side of the protein at pH 7 led to well resolved blockages of ionic current as shown in Figure 2b.

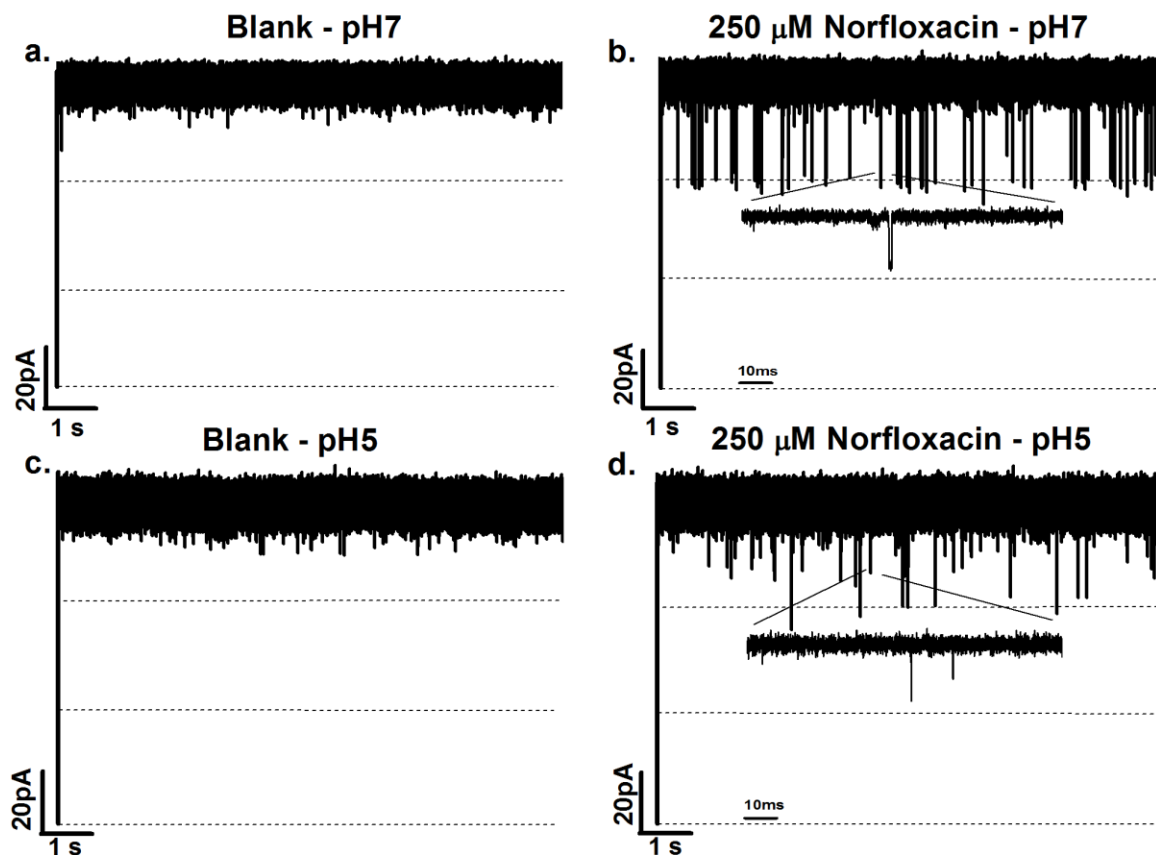


Figure 2. Ionic current traces of a single trimeric OmpF porin: (a) in the absence of antibiotics at pH 7, (b) with 250 μM norfloxacin *cis side* at pH 7, (c) in the absence of antibiotics at pH 5 and (d) with 250 μM norfloxacin *cis side* at pH 5. Electrolyte conditions: 1 M KCl, 5 mM acetate (pH 5) or 5 mM PO_4 (pH 7). The applied voltage was -25 mV. The dotted lines specify the ionic current levels through single monomers of the OmpF trimer. The addition of norfloxacin at pH 7 (b) leads to well resolved blockages of the ionic current through a monomer, whereas at pH 5 (d) the antibiotic molecules lead to flickering in the ionic current through a monomer – full blockages are not always observed. This is due to the low residence time of the antibiotic in the channel at pH 5, as discussed in the text.

At pH 5, the addition of 250 μM norfloxacin gave rise to partial unresolved flickering in the ionic current (Figure 2d); the ionic current through a monomer was not completely blocked due to the presence of the antibiotic. This was due to the low residence times of the norfloxacin molecules in the channel at pH 5, as discussed below.

The kinetic rate constants (association and dissociation rates) characterising the interaction of norfloxacin molecules with the OmpF channel were calculated as described previously²⁷; these are quantified in Table 1. Interestingly, the dissociation rate of the antibiotic varied by an order of magnitude at the different pH conditions. At pH 7 the residence time in the channel was about 900 μs (-25 mV experiments). However at pH 5, when the molecule is positively charged, this reduced to 40 μs (Table 1). This imbalance in the pH 7 and pH 5 residence times was observed at the higher transmembrane voltage of -50 mV as well (650 μs and 40 μs respectively). An obvious explanation suggests that the positive charge on the norfloxacin molecules at pH 5 results in them being driven through the porin under an applied transmembrane voltage. At pH 7 the overall charge on the molecule is neutral and thus the transmembrane voltage is less important; free diffusion is the primary driving agent. However, there might still be some small voltage

dependent effects since a significant proportion of the molecules are zwitterionic at pH 7 – this requires further investigation.

This interpretation seems validated by the flux values. The flux (J molecules/s) of norfloxacin through the channel was calculated based on a flux model valid for both symmetric and asymmetric transport through a channel²⁷⁻³⁰. When a transmembrane voltage of -25 mV was applied across the bilayer, the flux was found to be slightly higher at pH 5 (~ 2 molecules/s) than at pH 7 (~ 1 molecule/s). When the transmembrane voltage was increased to -50 mV, the norfloxacin flux value at pH 5 increased to 5 ± 1 molecules/s while the flux at pH 7 remained unchanged (1 molecule/s). This suggests that the positive charge on the norfloxacin molecule at pH 5 does influence its transport through the porin under an applied transmembrane voltage. Note that the flux was calculated using $\Delta c = 1$ mM, to compare with the optofluidic permeability assay results described above. This is justified since it was observed that the number of antibiotic events in the ionic current recordings increased linearly with an increasing concentration of the antibiotic, and hence the rate constants measured with a concentration difference of 250 μ M were equally applicable at a concentration difference of 1 mM.

Discussion

In this study, we used a label-free optofluidic permeability assay alongside single channel electrophysiology to explore the pH and voltage dependence of norfloxacin transport through OmpF porins. The optofluidic assay directly proves that the uptake of norfloxacin is enhanced by OmpF reconstituted in the proteoliposomes.

An interesting pattern emerges: in the absence of any transmembrane potential, the optofluidics assay shows that the flux per porin is essentially the same (within error) at both pH 5 and pH 7. However, as the transmembrane voltage is increased (electrophysiology), the flux at pH 5 starts to increase over the flux at pH 7. At a transmembrane voltage close to typical physiological OM Donnan potentials²¹ of -25 mV, the flux at pH 5 is twice as large as the flux at pH 7. On increasing the transmembrane voltage to -50 mV, the flux at pH 5 increases to five times that at pH 7. This confirms that the positive charge on norfloxacin at pH 5 contributes significantly to its transport across porins in the presence of transmembrane voltages.

It has been reported that a change in the pH from acidic to basic reduced the minimum inhibitory concentration (MIC) of norfloxacin¹⁷; furthermore, the antibiotic showed maximum cytoplasmic accumulation at pH 7.5¹⁸. This agrees well with the data obtained in our study. As mentioned above, our experiments suggest that norfloxacin will accumulate in the periplasm (across the porin) of an *E. coli* bacterium at a 2 \times faster rate at pH 5 compared to pH 7. However, the drug molecules now encounter the phospholipid inner membrane (IM). Our previous work showed that the direct diffusion of norfloxacin through a pure vesicle lipid bilayer is more effective (by a factor of approximately 6 \times) at pH 7 than at pH 5²⁵. Furthermore, the periplasmic pH is expected to be the same as the external pH³¹. Considering the relative rates of norfloxacin transport across the two membranes at pH 5 and pH 7 thus explains the higher cytoplasmic accumulation at neutral/slightly basic pH values^{17,18}. This suggests that diffusion through the inner membrane might present the rate limiting step. However, it should also be noted that medium acidification leads to the preferential expression of the narrower OmpC porins over OmpF²⁰ in *E. coli*, which might further reduce norfloxacin accumulation at acidic pH values.

Our analysis of norfloxacin transport through porins and lipids has thus clarified some of the mechanisms by which drug transport is affected under changing external conditions. The optofluidics assay also presents a direct visualisation of norfloxacin uptake across a proteoliposome membrane in a microfluidic, label-free system, not previously possible. The results unambiguously confirm the importance of these porins in facilitating the transport of fluoroquinolone antibiotics across the OM. In addition, our optofluidic technique enables the measurement of contributions to diffusion from pure lipids²⁵ and through porins, which cannot be done in a quantitative manner using the established liposome swelling assays^{7,32,33}. Furthermore, our microfluidic based approach has the potential to explore a wide range of porins. Proteoliposomes could be devised containing a combination of passive diffusion porins and active transporters, to study competition between these processes. New vesicle preparation techniques³⁴ have shown considerable promise for integration into lab-on-a-chip devices, which should translate into better control over porin insertions and proteoliposome modification. A combination of traditional and advanced single vesicle techniques can thus be used to investigate a variety of drug transport phenomena, an urgent need in medicine today.

Methods

Optofluidic Permeability Assay

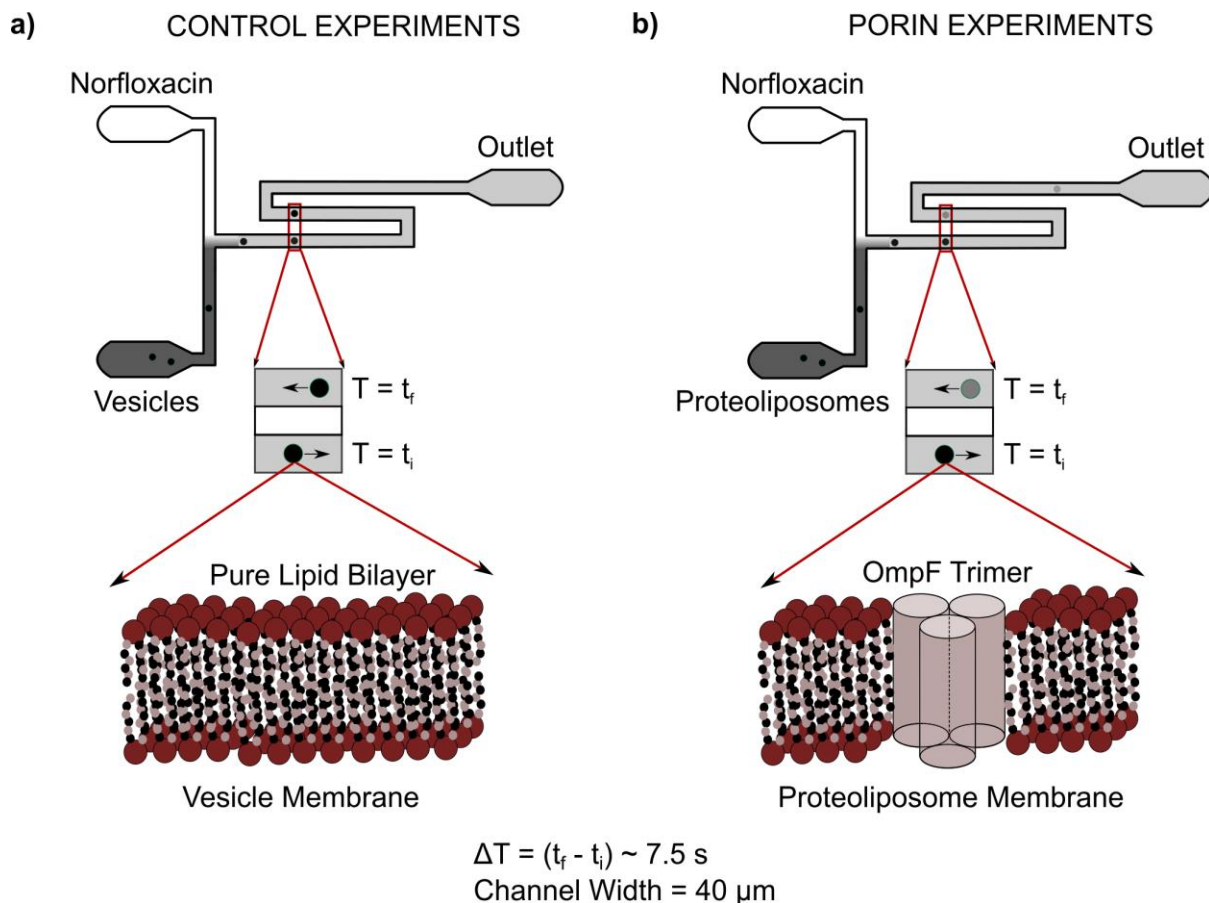


Figure 3. Schematic of the optofluidic permeability assay. Control experiments (no porin) are represented in a) and proteoliposome experiments (containing OmpF) in b). Vesicles (liposomes/proteoliposomes) are mixed with norfloxacin in a T junction microfluidic

chip by applying suction at the outlet reservoir with a syringe pump; norfloxacin autofluorescence is stimulated with a UV epifluorescence microscope. The vesicles are detected at an initial time t_i immediately post mixing and at a later time t_f , a distance of 7.4 mm further downstream. Vesicles took, on average, about 7.5 s to travel the intervening distance. Both time points are observed in the same field of view. Detection of the autofluorescence intensities within the vesicles at both points enables the calculation of the drug permeability coefficient for each vesicle.

The optofluidic permeability assay builds on our previous work studying the Permeability Coefficient of norfloxacin across lipid membranes²⁵. It was designed to explore properties of porin mediated transport not accessible to electrophysiology and other traditional techniques. It enables the study of drug transport through porins without the application of a transmembrane voltage. Furthermore, even though electrophysiology has been the method of choice for characterising antibiotic-porin interactions at the single molecule level³⁵⁻³⁸, it suffers from an inability to distinguish molecules that translocate through the porin from molecules that simply bind transiently²⁷. The optofluidic permeability assay visualises drug transport directly, by observing the drug molecules themselves via their autofluorescence; it is thus label-free. Liposome swelling assays^{32,33} were previously used as an alternative to electrophysiology. However, these measure antibiotic flux relative to the flux of a permeable sugar (generally arabinose) and hence cannot measure drug permeability directly. Furthermore, the diffusion of charged compounds in these assays is influenced by the build-up of Donnan potentials inside the liposomes, which can lead to unexpected osmotic behaviour³². Our assay overcomes many of these intrinsic limitations and provides a new technique for studies of drug transport with porins.

As described in Figure 3, the optofluidic permeability assay involves a T junction microfluidic chip where the vesicles (liposomes/proteoliposomes) and the drug molecules are mixed in a channel (via the application of suction at the outlet). The T junction geometry of the chip leads to an equal mixing of vesicle and drug solutions. The inlet norfloxacin concentration is 2 mM (prepared in the same buffer solution as the vesicles) and hence the vesicles are exposed to a final norfloxacin concentration of 1 mM. The vesicles are imaged immediately post mixing with the norfloxacin and at a distance 7.4 mm further along the channel; the chip was designed such that both points were observed in the same field of view (Figure 3). The chip design was based on preliminary experiments which showed that a distance of about 7-8 mm between the two points was optimal for the detection of proteoliposomes showing increased uptake of the drug.

The norfloxacin molecules were tracked by stimulating their autofluorescence in the UV²⁵. We performed all the optofluidics experiments described in this paper on a commercial Olympus IX73 microscope, using a DAPI filter set (Chroma) and a Mercury arc lamp (Prior Lumen 200). A 60x air objective was used (Olympus LUCPlanFLN, NA 0.70). Images were recorded using a scientific CMOS camera (optiMOS, QImaging) which enabled recording at 100 fps (10 ms exposure, bin 4). The microfluidic flows were controlled using a neMESYS syringe pump with a 250 μ l Duran Borosilicate glass syringe (ILS, Germany) connected to the outlet. At the beginning of the experiments, a flow of 30-40 μ l/hr was applied until the autofluorescence intensity in the microfluidic channel reached its peak, ensuring an appropriate drug concentration in the channel. Once this level was reached, the flow was slowed to 3 μ l/hr enabling the detection of individual vesicles for multiple frames as desired²⁵.

The images were recorded using Micromanager 1.4³⁹ and analysed in MATLAB (scripts available on request) to obtain information about the autofluorescence intensities within the vesicles, in addition to the background intensity, vesicle shape and velocity²⁵. Upchurch 1520 G tubing (inner diameter 0.03 inch) was used to connect the outlet of the chip to the syringe. Full details of the

mathematical model and permeability coefficient calculations can be found in the earlier paper²⁵. Calculations of the flux are presented in the Supplementary Information document.

Microfluidic Chip Fabrication

The microfabrication of the fluidic chip relies on photolithography and replica molding. For the fabrication of the mold, a Silicon substrate was covered with a thin layer of adhesion promoter (Omnicoat, Microchem, spin coating: 2,000 r.p.m., 30 sec). A layer of SU-8 2025 (Microchem) was then deposited (2,000 r.p.m., 30 s), pre-baked (2 min at 65 °C, 5 min at 95 °C) and selectively exposed to ultraviolet light (12 s, 365-405 nm, 20 mWcm⁻²) through a bespoke pellicle mask (Photodata Ltd, CAD file available on request). The sample was post-baked (1 min at 65 °C, 3 min at 95 °C), developed for 3 min, dried with a gentle stream of Nitrogen and hard baked for 5 min at 95 °C.

Sylgard 184 polydimethylsiloxane (PDMS) was used to create a negative replica from the Silicon mold using standard soft lithography techniques⁴⁰ with an elastomer:curing agent ratio of 9:1 (Dow Corning). The PDMS mixture was poured onto the Silicon mold and baked at 60 °C for 55 minutes. The PDMS chip was then peeled off the mold and inlet/outlet columns created using a 1.5 mm biopsy punch (Miltex). The chip was plasma bonded to a glass coverslip (Type I, Assistant, Germany) using an air plasma (10 W, 25 sccm, 10 s exposure, Diener, Royal Oak, MI). Post plasma bonding, the chip was left in an oven at 60 °C for 5-10 minutes to enhance the adhesion of PDMS to glass.

Vesicle formation and OmpF incubation

Giant Unilamellar Vesicles (GUVs) of 1,2-diphytanoyl-*sn*-glycero-3-phosphocholine (DPhPC) lipids (Avanti Polar Lipids) were prepared via electroformation using a Nanion Vesicle Prep Pro (Nanion Technologies GmbH, Germany) setup as described previously²⁵. The GUVs were prepared in 200 mM Sucrose with 5 mM Phosphate Buffer (pH 7) or 5 mM Acetic Acid (pH 5).

The OmpF incubation followed previously established protocols⁴¹. Purified stock OmpF (5.5 mg/ml) in a detergent, a 1% solution of n-Octylpolyoxyethylene (octyl-POE, Bachem) prepared in Milipore water, was diluted 1:1 in the same detergent and vortexed; 1 µl of this freshly diluted OmpF solution was added to 199 µl of the vesicle stock solution and incubated at room temperature for an hour. Biobeads[®] SM-2 (Bio-Rad) were added to remove the detergent and the mixture was incubated at room temperature for 45-60 minutes followed by storage at 4 °C overnight. The next day, the OmpF embedded proteoliposome solution was separated from the Biobeads with a pipette and the sample used directly in experiments. For the control (liposome) experiments, 1 µl of 1% octyl-POE (instead of the OmpF solution) was added to 199 µl of the vesicles; the rest of the incubation protocol remained unchanged.

Single OmpF porin ionic current measurements in a solvent-free lipid bilayer

Reconstitution experiments and noise analyses were performed as described in detail previously⁴². The Montal and Mueller technique⁴³ was used to form a phospholipid bilayer using DPhPC (Avanti polar lipids). A Teflon film comprising an aperture of approximately 30-60 µm in diameter was placed between the two chambers of a cuvette. The aperture was pre-painted with 1% hexadecane in hexane for stable bilayer formation. 1 M KCl in 5 mM potassium acetate (pH 5) or 5 mM phosphate (pH 7) was used as the electrolyte solution and added to both sides of the chamber. Ionic currents were detected using standard silver-silver chloride electrodes from WPI (World Precision Instruments) that were inserted in both sides of the cuvette. Single channel

measurements were performed by adding the protein to the *cis* side of the chamber (the side connected to the ground electrode). Spontaneous channel insertion was typically obtained while stirring the solution in the cuvette under an applied transmembrane voltage. After a successful single channel reconstitution, the *cis* side of the chamber was carefully perfused to remove any remaining porins, thus preventing further channel insertions. Conductance measurements were performed using an Axopatch 200B amplifier (Molecular Devices) in voltage clamp mode. Signals were filtered by an on-board low pass Bessel filter at 10 kHz with a sampling frequency of 50 kHz. Amplitude, probability and noise analyses were performed using OriginPro 8 (OriginLab) and Clampfit software (Molecular Devices). Single channel analysis was used to determine the antibiotic binding kinetics. In a single channel measurement, the quantities measured were the duration of blocked levels/residence times (τ_c) and the frequency of blockage events (ν). The association rate constant k_{on} was derived using the number of blockage events, $k_{on} = \nu/3[c]$, where $[c]$ is the concentration of the antibiotic. The dissociation rate constant (k_{off}) was determined by averaging the $1/\tau_c$ values recorded over the entire concentration range³⁸.

Port-a-Patch

Planar lipid bilayers were obtained from GUVs prepared using the same electroformation protocol described earlier. Purified stock OmpF (5.5 mg/ml) porins in 1% octyl-POE were diluted in the detergent and reconstituted into GUVs by incubating the porins as described previously; however, the final porin concentrations used in the Port-a-Patch calibration experiments were a factor of 500 \times , 250 \times and 100 \times more dilute than the final concentration used in the optofluidics assay to enable the counting of single porin insertions in the ionic current traces. After incubation, the detergent was removed using Biobeads[®] SM-2 (Bio-Rad) as described previously. The Biobeads were discarded after centrifugation and the protein containing GUVs (proteoliposomes) used immediately.

For the formation of a planar lipid bilayer containing the proteins, 5 μ l of the proteoliposome solution was pipetted into 5 μ l of the electrolyte solution (200 mM KCl, 5 mM acetic acid for pH 5 or 5 mM phosphate for pH 7). The resulting solution was placed on a microstructured glass chip (grounded side) containing an aperture approximately 1 μ m in diameter. The vesicles burst once they touch the glass surface of the chip thus forming a planar lipid bilayer; additional suction was applied to patch GUVs across the aperture. Ionic current measurements were performed using the same equipment and software as for the black lipid membrane measurements described above.

Acknowledgements

This work was supported by a European Research Council (ERC) Grant (261101 Passmembrane) to UFK. JC acknowledges support from an Internal Graduate Studentship, Trinity College, Cambridge, and a Research Studentship from the Cambridge Philosophical Society. SP was supported by the Leverhulme Trust through an Early Career Fellowship. TM acknowledges support from the Konrad-Adenauer Foundation and the German National Merit Foundation. HB, YB and MW are part of the TRANSLOCATION consortium and have received support from the Innovative Medicines Joint Undertaking under grant agreement 115525, the European Union's seventh framework program (FP7/2007-2013), and European Federation of Pharmaceutical Industries and Associates companies in-kind contribution. We thank Avelino Javier for help with the MATLAB scripts and Catalin Chimerele for helpful discussions.

Author Contributions

JC and HB contributed equally to this work. JC, HB, SP, TM and YB performed the experiments. JC, HB, SP, MW and UFK planned the project. JC, HB, SP, MW and UFK wrote the paper.

All data accompanying this publication are directly available within the publication.

Financial Interests

The authors declare no competing financial interests.

References

1. Allen, H. K., et al. Call of the wild: antibiotic resistance genes in natural environments. *Nat. Revs. Microbiol.***8**, 251-259 (2010).
2. Cantas, L., et al. A brief multi-disciplinary review on antimicrobial resistance in medicine and its linkage to the global environmental microbiota. *Frontiers in Microbiol.***4**, 1-14 (2013).
3. McKenna, M. The Last Resort. *Nature*, **499**, 394-396 (2013).
4. Davies, J. & Davies, D. Origins and Evolution of Antibiotic Resistance. *Microbiol. and Mol. Biol. Revs.***74**, 417-433 (2010).
5. Ling, L. L., et al. A new antibiotic kills pathogens without detectable resistance. *Nature*, **517**, 455-459 (2015).
6. Delcour, A. H. Outer Membrane Permeability and Antibiotic Resistance. *Biochim. Biophys. Acta*, **1794** (5), 808-816 (2009).
7. Pagès, J-M., James, C. E. & Winterhalter, M. The porin and the permeating antibiotic: a selective diffusion barrier in Gram-negative bacteria. *Nat. Revs. Microbiol.***6**, 893-903 (2008).
8. Redgrave, L. S., Sutton, S. B., Webber, M. A. & Piddock, L. J. V. Fluoroquinolone resistance: mechanisms, impact on bacteria, and role in evolutionary success. *Trends in Microbiol.*, **22**(8), 438-445 (2014).
9. Chevalier, J., Malléa, M. & Pagès, J-M. Comparative aspects of the diffusion of norfloxacin, cefepime and spermine through the F porin channel of *Enterobacter cloacae*. *Biochem. J.*, **348**, 223-227 (2000).
10. Hirai, K., et al. Isolation and Characterization of Norfloxacin-Resistant Mutants of *Escherichia coli* K-12. *Antimicrob. Agents Chemother.*,**30**, 248-253 (1986).
11. Cohen, S. P., McMurry, L. M., Hooper, D. C., Wolfson, J. S. & Levy, S. B. Cross-Resistance to Fluoroquinolones in Multiple Antibiotic-Resistant (Mar) *Escherichia coli* Selected by Tetracycline or Chloramphenicol: Decreased Drug Accumulation Associated with Membrane Changes in Addition to OmpF Reduction. *Antimicrob. Agents Chemother.*, **33**, 1318-1325 (1989).
12. Kishii, R. & Takei, M. Relationship between the expression of *ompF* and quinolone resistance in *Escherichia coli*. *J. Infect. Chemother.*,**15**, 361-366 (2009).
13. Stavenger R. A & Winterhalter M. TRANSLOCATION Project: How to Get Good Drugs into Bad Bugs. *Sci. Transl. Med.*, **6**, 228ed7 (2014).
14. Hooper, D. C. Mechanisms of Action of Antimicrobials: Focus on Fluoroquinolones. *Clin. Infect. Dis.*, **32** (Suppl. 1), S9-S15 (2001).
15. Zeiler, H. J. Evaluation of the in vitro bactericidal action of ciprofloxacin on cells of *Escherichia coli* in the logarithmic and stationary phases of growth. *Antimicrob. Agents Chemother.*,**28**, 524–527(1985).

16. Hooper, D. C., Wolfson, J. S., Souza, K. S., Ng, E. Y., McHugh, G. L. & Swartz, M. N. Mechanisms of quinolone resistance in *Escherichia coli*: characterization of *nfxB* and *cfxB*, two mutant resistance loci decreasing norfloxacin accumulation. *Antimicrob. Agents Chemother.* **33**, 283–290 (1989).
17. Smith, J. T. & Ratcliffe, N. T. Effect of pH value and magnesium on the antibacterial activity of quinolone preparations. *Infection*, **14 Suppl 1**, S31–35 (1986).
18. Nikaido, H. & Thanassi, D. G. Penetration of Lipophilic Agents with Multiple Protonation Sites into Bacterial Cells: Tetracyclines and Fluoroquinolones as Examples. *Antimicrob. Agents Chemother.*, **37**, 1393-1399 (1993).
19. Piddock, L. J. V., Jin, Y.-F., Ricci, V. & Asuquo, A. E. Quinolone accumulation by *Pseudomonas aeruginosa*, *Staphylococcus aureus* and *Escherichia coli*. *J. Antimicrob. Chemother.*, **43**, 61-70 (1999).
20. Thomas, A. D. & Booth, I. R. The regulation of expression of the porin gene *ompC* by acid pH. *J. Gen. Microbiol.*, **138**, 1829-1835 (1992).
21. Sen, K., Hellman, J. & Nikaido, H. Porin Channels in Intact Cells of *Escherichia coli* Are Not Affected by Donnan Potentials Across the Outer Membrane. *J. Biol. Chem.*, **263 (3)**, 1182-1187 (1988).
22. Kennedy, E. P. Osmotic regulation and the biosynthesis of membrane-derived oligosaccharides in *Escherichia coli*. *Proc. Nat. Acad. Sci. USA*, **79**, 1092-1095 (1982).
23. Mortimer P. G. & Piddock, L. J. A comparison of methods used for measuring the accumulation of quinolones by *Enterobacteriaceae*, *Pseudomonas aeruginosa* and *Staphylococcus aureus*. *J. Antimicrob. Chemother.* **38**, 639-653 (1991).
24. Kaščáková, S., Maigre, L., Chevalier, J., Réfrégiers, M. & Pagès, J. M. Antibiotic transport in resistant bacteria: Synchrotron UV fluorescence microscopy to determine antibiotic accumulation with single cell resolution. *PLOS ONE* **7**, e38624 (2012).
25. Cama, J., Chimerel, C., Pagliara, S., Javer, A. & Keyser, U. F. A label-free microfluidic assay to quantitatively study antibiotic diffusion through lipid membranes. *Lab Chip*, **14**, 2303-2308 (2014).
26. Angelova, M. I. & Dimitrov, D. S. Liposome Electroformation. *Faraday Discuss. Chem. Soc.*, **81**, 303-311 (1986).
27. Mahendran, K. R., et al. Molecular Basis of Enrofloxacin Translocation through OmpF, an Outer Membrane Channel of *Escherichia coli* – When Binding Does Not Imply Translocation. *J. Phys. Chem. B*, **114**, 5170–5179 (2010).
28. Benz, R., Schmid, A. & Vos-Scheperkeuter, G. H. Mechanism of sugar transport through the sugar-specific LamB channel of *Escherichia coli* outer membrane. *J. Membr. Biol.* **100(1)**, 21–29 (1987).
29. Schwarz, G., Danelon, C. & Winterhalter, M. On Translocation Through a Membrane Channel via an Internal Binding Site: Kinetics and Voltage Dependence. *Biophys. J.*, **84**, 2990-2998 (2003).
30. Bezrukov, S. M., Berezhkovskii, A. M. & Szabo, A. Diffusion model of solute dynamics in a membrane channel: Mapping onto the two-site model and optimizing the flux. *J. Chem. Phys.*, **127**, 115101 (2007).
31. Wilks, J. C. & Slonczewski, J. L. pH of the cytoplasm and periplasm of *Escherichia coli*: rapid measurement by green fluorescent protein fluorimetry. *J. Bacteriol.* **189**, 5601–5607 (2007).
32. Nikaido, H. & Rosenberg, E. Y. Porin channels in *Escherichia coli*: studies with liposomes reconstituted from purified proteins. *J. Bacteriol.* **153**, 241–252 (1983).

33. Yoshimura, F. & Nikaido, H. Diffusion of beta-lactam antibiotics through the porin channels of *Escherichia coli* K-12. *Antimicrob. Agents Chemother.* **27**, 84–92(1985).
34. Karamdad, K., Law, R. V., Seddon, J. M., Brooks, N. J. & Ces, O. Preparation and mechanical characterisation of giant unilamellar vesicles by a microfluidic method. *Lab Chip*, **15**, 557-562 (2015).
35. Delcour, A. H. Function and modulation of bacterial porins: insights from electrophysiology. *FEMS Microbiol. Lett.*, **151**, 115-123 (1997).
36. Delcour, A. H., Martinac, B., Adler, J. & Kung, C. Modified reconstitution method used in patch-clamp studies of *Escherichia coli* ion channels. *Biophys. J.*, **56**, 632-636 (1989).
37. Buechner, M., Delcour, A. H., Martinac, B., Adler, J. & Kung, C. Ion channel activities in the *Escherichia coli* outer membrane. *Biochim. Biophys. Acta*, **1024**, 111-121 (1990).
38. Nestorovich, E. M., Danelon, C., Winterhalter, M. & Bezrukov, S. M. Designed to penetrate: Time-resolved interaction of single antibiotic molecules with bacterial pores. *Proc. Nat. Acad. Sci. USA*, **99**, 9789-9794 (2002).
39. Stuurman, N., Amdodaj, N. & Vale, R. μ Manager: Open Source Software for Light Microscope Imaging. *Microscopy Today*, **15**, 42-43 (2007).
40. Qin, D., Xia, Y. & Whitesides, G. M. Soft lithography for micro- and nanoscale patterning. *Nat. Protocols*, **5**, 491-502 (2010).
41. Kreir, M., Farre, C., Beckler, M., George, M. & Fertig, N. Rapid screening of membrane protein activity: electrophysiological analysis of OmpF reconstituted in proteoliposomes. *Lab Chip*, **8**, 587-595 (2008).
42. Singh, P. R., Ceccarelli, M., Lovelle, M., Winterhalter, M. & Mahendran, K. R. Antibiotic Permeation across the OmpF Channel: Modulation of the Affinity Site in the Presence of Magnesium. *J. Phys. Chem. B*, **116**, 4433-4438 (2012).
43. Montal, M. & Mueller, P. Formation of Bimolecular Membranes from Lipid Monolayers and a Study of their Electrical Properties. *Proc. Nat. Acad. Sci. USA*, **69**, 3561-3566 (1972).

Table 1: Antibiotic association (k_{on}) and dissociation (k_{off}) rate constants obtained by single channel measurements for OmpF at pH 5 and pH 7. Electrolyte conditions: 1 M KCl, 5 mM PO₄ (pH 7)/acetate (pH 5).

$$k_{on} = (\text{No. of events/sec}) / 3 \cdot [c], \quad k_{off} = (1/\text{residence time})$$

$$J = \frac{k_{on}^{cis} \cdot c_{cis} \cdot k_{on}^{trans}}{(k_{on}^{cis} + k_{on}^{trans})}; \quad \Delta c = 1 \text{ mM: valid under } k_{off} \gg k_{on} \cdot c$$

Antibiotics	k_{on}^{cis} (10 ³) {1/(s·M)}	k_{on}^{trans} (10 ³) {1/(s·M)}	k_{off}^{total} 1/(s)	J (molecules/s)
Norfloxacin	-50mV	+50mV		$\Delta c = 1 \text{ mM}$
pH 7	13 ± 5	1.3	1561 ± 120	1
pH 5	11 ± 3	10	25000	5 ± 1
	-25mV	+25mV		
pH 7	9 ± 2.5	1	1150 ± 60	0.9
pH 5	3 ± 1	5 ± 2	27000	1.8 ± 0.7
	0 mV (Optofluidics)			
pH 7				10 ± 7
pH 5				14 ± 9

Errors are standard deviations.

Table of Contents Graphic

